Published in final edited form as:
J Immunol. 2008 June 1; 180(11): 7471–7479.

Autoimmune Disease-Associated Alleles Affect Histamine Receptor H_1 Protein Trafficking and Cell Surface Expression

Rajkumar Noubade[*], **Naresha Saligrama**[*], **Karen Spach**[*], **Roxana del Rio**[*], **Elizabeth P. Blankenhorn**[†], **Theodoros Kantidakis**[‡], **Graeme Milligan**[‡], **Mercedes Rincon**[*], and **Cory Teuscher**[*,§]

* *Departments of Medicine and Pathology, University of Vermont, Burlington, VT 05405*

† *Department of Microbiology and Immunology, Drexel University College of Medicine, Philadelphia, PA 19129*

‡ *Molecular Pharmacology Group, Institute of Biomedical and Life Sciences, University of Glasgow, Glasgow G12 8QQ Scotland, UK*

Abstract

Structural polymorphisms (L263P, M313V and S331P) in the third intracellular loop of the murine histamine receptor H_1 (H_1R) are candidates for *Bphs*, a shared autoimmune disease locus in experimental allergic encephalomyelitis (EAE) and experimental allergic orchitis. The P-V-P haplotype is associated with increased disease susceptibility (H_1R^S) whereas the L-M-S haplotype is associated with less severe disease (H_1R^R). Here we show that selective reexpression of the H_1R^S allele in T cells fully complements EAE susceptibility and the production of disease associated cytokines while selective reexpression of the H_1R^R allele does not. Mechanistically, we show that the two H_1R alleles exhibit differential cell surface expression and altered intracellular trafficking, with the H_1R^R allele being retained within the endoplasmic reticulum (ER). Moreover, we show that all three residues (L-M-S) comprising the H_1R^R haplotype are required for altered expression. These data are the first to demonstrate that structural polymorphisms influencing cell surface expression of a G-protein coupled receptor in T cells regulates immune functions and autoimmune disease susceptibility.

Keywords

Histamine receptor 1; EAE/MS; GPCR; receptor trafficking; autoimmunity

§To whom correspondense should be addressed at : C317 Given Medical Building University of Vermont, Burlington, VT 05405, (802) 656-3270, C.Teuscher@uvm.edu.

INTRODUCTION

Multiple sclerosis (MS) is the major demyelinating disease of the central nervous system (CNS) in humans, affecting more than 2.5 million people worldwide (1). Both environmental and genetic factors contribute to the immunopathologic etiology of the disease. A genetic component in disease susceptibility is supported by the 20–30% concordance rate among monozygotic twins and 3–5% for dizygotic twins. Compared to the general population, MS is 20–40 times more common in first degree relatives and there is no excess risk in adopted relatives of patients with MS (2). Evidence of an environmental etiology in MS comes primarily from migration studies and geographic distribution data. Migration studies indicate that individuals moving from high-risk areas before puberty tend to adopt the lower risk of the native population and vice versa (3). Thus, susceptibility to MS is likely the result of environmental triggers acting on a susceptible genetic background at the population level.

Experimental allergic encephalomyelitis (EAE), the primary animal model of MS, is also a genetically determined inflammatory disease of the CNS (4). EAE can be actively induced in genetically susceptible animals by immunization with either whole spinal cord homogenate or encephalitogenic proteins/peptides and adjuvants (5). EAE, like MS, is a complex polygenic disease (6), with multiple genes exerting a modest effect, thus making it difficult to study the contribution of individual loci to overall disease pathogenesis. However, reduction of complex disease states into intermediate or subphenotypes that are under the control of a single locus has the potential to facilitate mechanistic studies and gene identification (6). One such phenotype associated with EAE is *Bordetella pertussis* toxin-induced histamine sensitization, which is controlled by the single autosomal dominant locus known as *Bphs* (7). Previously, we identified *Hrh1*/H_1R as the gene underlying *Bphs* (7) and as a shared autoimmune disease susceptibility gene in EAE (8) and experimental allergic orchitis (EAO) (9). H_1R is a seven-transmembrane spanning, G protein coupled receptor (GPCR). Generally, ligation of H_1R with histamine is believed to couple to second messenger signaling pathways via the activation of the heterotrimeric $G\alpha_{q/11}$ family of G proteins and leads to a variety of signaling cascades depending on the cell type involved (10).

Compared to wild-type (WT) mice, H_1R deficient (H1RKO) mice exhibit significantly reduced EAE susceptibility (7). As a disease susceptibility gene, *Hrh1*/H_1R can exert its effect in multiple cell types involved in the disease process including endothelial cells, antigen presenting cells and T cells. Moreover, H_1R may function at critical check points during both the induction and effector phases of the disease. In this regard, we recently demonstrated that selective reexpression of the H_1R^S allele in T cells is sufficient to complement EAE in H1RKO mice and that H_1R signals are important during priming of naïve T cells rather than during the effector phase of the disease (11).

Hrh1/H_1R-susceptible (*Hrh1*^{S}/H_1R^S) and –resistant (*Hrh1*^{R}/H_1R^R) alleles differ by three amino acids in their coding sequences (7). The H_1R^R haplotype possesses a L^{263}, M^{313} and S^{331} whereas the H_1R^S haplotype is characterized by P^{263}, V^{313} and P^{331} (7). The mechanism whereby these polymorphic residues influence EAE susceptibility is unknown but it was hypothesized to be the result of differential coupling to second messenger signaling pathways, because the three residues reside within the third intracytoplasmic domain associated with $G\alpha_{q/11}$ activation (12). Here we show that, unlike the H_1R^S allele (11), expression of the H_1R^R allele in T cells does not complement EAE in H1RKO mice and that the polymorphic residues of the H_1R^R allele affect intracellular trafficking and retention in the ER rather than the inherent capacity to signal. Moreover, we show that all three residues (L-M-S) comprising the H_1R^R haplotype are required for altered cell surface expression. These data are the first to demonstrate that structural polymorphisms influencing differential cell surface expression of a GPCR in T cells can regulate immune functions and susceptibility to autoimmune disease.

MATERIALS AND METHODS

Mice

C57BL/6J mice were purchased from the Jackson Laboratory (Bar Harbor, ME). B6.129P-*Hrh1*^{tm1Wat} (H1RKO) (13) mice were maintained in the animal facility at the University of Vermont (Burlington, VT). The experimental procedures used in this study were approved by the Animal Care and Use Committee of the University of Vermont.

For transgenic mouse generation, the HA-H_1R^S or HA-H_1R^R constructs were made by deleting the methionine of the *Bphs*-susceptible H_1R allele from SJL/J and *Bphs*-resistant C3H/HeJ mice, respectively (7), and adding an HA tag at the N-terminus using TOPO cloning vector (Invitrogen, Carlsbad, CA). The HA-H_1R was then subcloned downstream of the distal *lck* promoter (14). The linear DNA fragment containing the distal *lck* promoter, the HA-H_1R gene and the human growth hormone (hGH) intron and polyadenylation signal was injected directly into fertilized C57BL/6J eggs at the University of Vermont transgenic/knockout facility. Mice were screened by DNA slot blot testing using a *Bam*HI–*Sac*I 0.5 kb fragment from the *hGH* gene as a probe. Two founders were generated for both the H_1R^S and H_1R^R alleles and each was crossed to H1RKO mice to establish transgenic mouse lines on the H1RKO background (H1RKO-Tg^S1 and H1RKO-Tg^S2 and H1RKO-Tg^R1 and H1RKO-Tg^R2 mice). Mice from the H1RKO-Tg^S1 line expressed the transgene at comparable levels to the two lines expressing the $H1R^R$ allele, so it was used in all the experiments in this study.

Cytokine production

For cytokine analysis spleen and lymph nodes were obtained from mice immunized ten days earlier with either $MOG_{35–55}$-CFA plus PTX or 2× $MOG_{35–55}$-CFA model, single cell suspensions prepared at a concentration of 1×10^6 cells/ml in RPMI medium and stimulated with 50 μg/ml of $MOG_{35–55}$. Cell culture supernatants were recovered at 72 h and cytokine levels measured by ELISA using anti-IFN-γ, anti-IL-4 and anti-IL17 mAbs and their corresponding biotinylated mAbs (BD Pharmingen, San Diego, CA). TNF-α ELISA kit was from (BD Pharmingen, San Diego, CA).

Proliferation Assays

Mice were immunized with the 2× $MOG_{35–55}$-CFA protocol: single cell suspensions were prepared at 2.5×10^5 cells/well in RPMI medium and stimulated in a 96 well plate with different concentrations (0, 2, 10 and 50 μg/ml) of $MOG_{35–55}$ for 72 h and proliferation was determined by [^{3}H]-thymidine incorporation during the last 18 h of culture.

Cell surface expression studies

The pEGZ-HA vector plasmid was a generous gift from Dr. Ingolf Berberich (University of Wurzburg, Wurzburg, Germany). Two restriction sites, *BamHI* and *EcoRI* were inserted into H_1R^S or H_1R^R cDNA by PCR and cloned such that the second codon is in-frame with the HA tag of pEGZ generating an HA-H_1R fusion protein. pEGZ is a bicistronic system with IRES-EGFP. EGFP served as a marker for transfected cells.

HEK293T cells were plated at 1.25×10^6 cells/plate and cultured in DMEM-F12 containing 10% FBS. When the cells were about 50–80% confluent, they were transfected with 5 μg of pEGZ-HA-H_1R^S, pEGZ-HA-H_1R^R or the empty pEGZ vector using calcium phosphate method. After 16–24 h, cells were scraped off the plate by rigorous pipetting with 1% Calf serum in PBS and stained with anti-HA mAb conjugated to PE (Miltenyi Biotech, Auburn, CA) according to the manufacturer's guidelines. Cells were analyzed by Flow cytometry using FACSAria instrument (BD Pharmingen, San Diego, CA) and the data were further analyzed using FlowJo flow cytometry analysis software (Tree star Inc, Ashland, OR).

Confocal microscopy

HEK293T cells were transfected with pEGA-HA-H_1R^S, pEGZ-HA-H_1R^R or empty pEGZ control vector (5 μg total DNA) using the calcium phosphate method. Cells were fixed, permeabilized and stained using an anti-HA mAb (Cell Signaling Technologies, Danvers, MA) followed by an incubation with Alexa-568 anti-mouse antibody (Molecular Probes, Eugene, Oregon). TOPRO-3 nuclear stain (Molecular Probes, Eugene, Oregon) was used as a nuclear marker. For non-permeabilized cells, the transfected HEK293T cells were stained with the anti-HA mAb and were then fixed. Cells were examined by confocal microscopy using Zeiss LSM 510 META Confocal Laser Scanning Imaging System (Carl Ziess Microimaging Inc, Thronwood, NY).

Cell lysates and Western blotting

Whole-cell lysates were prepared from HEK293T cells transfected with various pEGZ constructs in Triton lysis buffer and were then separated via sodium dodecyl sulfate-polyacrylamide gel electrophoresis (SDS-PAGE) and transferred to nitrocellulose membranes as described previously (11). Anti-HA mAb (Abcam Inc. Cambridge, MA) was used as primary antibody. Anti-actin (Santa Cruz Biotechnology, Santa Cruz, CA) was used as a loading control.

[^{3}H]mepyramine binding studies

[^{3}H]mepyramine binding studies were conducted as described (15) and were used to measure expression levels of H_1R variants and the H_1R^S-$G\alpha_{q/11}$ and H_1R^R-$G\alpha_{q/11}$ fusion proteins.

[^{35}S]GTPγS binding Assay

[^{35}S]GTPγS binding experiments to assess the capacity of H_1R variants to cause activation of $G\alpha_{q/11}$ were initiated by the addition of cell membranes containing 50 fmols of H_1R variant constructs to assay buffer (20mM HEPES (pH 7.4), 3mM $MgCl_2$, 100mM NaCl, 1μM GDP, 0.2mM ascorbic acid, and 100nCi [^{35}S]GTPγS) containing 100μM histamine. Non-specific binding was determined in the above condition with the addition of 100μM GTPγS. Reactions were incubated for 15 min at 30° C and were terminated by the addition of 500μl of ice-cold buffer containing 20mM HEPES (pH 7.4), 3mM $MgCl_2$, 100mM NaCl and 0.2mM ascorbic acid. The samples were centrifuged at 16,000 × g for 10 min at 4° C. The resulting pellets were re-suspended in solubilization buffer (100mM Tris, 200mM NaCl, 1mM EDTA, and 1.25% Nonidet P-40) plus 0.2% SDS. Samples were precleared with Pansorbin for 1 h, followed by immunoprecipitation with a C-terminal anti- $G\alpha_q/G_{\alpha 11}$ antiserum (16). Finally, the immunocomplexes were washed with solubilization buffer and bound [^{35}S]GTPγS was estimated by liquid scintillation-spectrometry.

Site directed mutagenesis

pEGZ-HA-H_1R^S was used as template to generate single H_1R^S mutants with each of the polymorphic residues replaced with the corresponding residue of the H_1R^R allele using the Quickchange (Strategene) site directed mutagenesis kit, according to the manufacturer's guidelines. The forward primers used for the mutagenesis were: for P263L 5′-GGGGGTCCAGAAGAGG**CCG**TCAAGAGACCCTACTGG-3′, for V312M 5′-CATGCAGACACAGCC**TGT**GCCTGAGGGAGATGCCAGG-3′, for P330S 5′-CCAGACCTTGAGCC**AGC**CCAAAATGGATGAGCAGAGC-3′. The reverse primers were the complementary sequences of these primers. The altered nucleotides are shown in bold and underlined. The mutants were sequence confirmed and were used as template for the generation of different combinations of double H_1R^S mutants.

Conventional and Quantitative Real-Time Polymerase Chain Reaction (RT-PCR)

Total RNA was extracted from CD4 T cells using RNeasy RNA isolation reagent (Qiagen, Valencia, CA) as recommended by the manufacturer. cDNA generated from 1 μg total RNA was used in conventional and quantitative real-time RT-PCR as described earlier (11).

Induction and Evaluation of EAE

Mice were immunized for the induction of EAE using either the $MOG_{35–55}$-complete Freund's adjuvant (CFA) double-inoculation (2× $MOG_{35–55}$-CFA) (17) or the $MOG_{35–55}$-CFA plus PTX single-inoculation ($MOG_{35–55}$-CFA plus PTX) protocols (18). For the 2× $MOG_{35–55}$-CFA induction protocol mice are injected subcutaneously with an emulsion of 100 μg of $MOG_{35–55}$ and an equal volume of CFA containing 200 μg of *Mycobacterium tuberculosis* H37RA (Difco Laboratories, Detroit, MI) in the posterior right and left flank; one week later all mice were similarly injected at two sites on the right and left flank anterior of the initial injection sites. Animals immunized using the $MOG_{35–55}$-CFA plus PTX single-inoculation protocol received an emulsion of 200 μg $MOG_{35–55}$ and equal volume of CFA containing 200 μg of *Mycobacterium tuberculosis* H37RA by subcutaneous injections distributed equally in the posterior right and left flank and scruff of the neck. Immediately thereafter, each animal received 200 ng PTX (List Biological Laboratories, Campbell, CA) by intravenous injection. Mice were scored daily starting at day 5 post-injection as previously described (18). Clinical quantitative trait variables including disease incidence and mean day of onset (DO), cumulative disease score (CDS), number of days affected (DA), overall severity index (SI) and the peak score (PS) were generated as previously described (17).

Statistical analysis

Statistical analyses, as detailed in the figure legends, were performed using GraphPad Prism 4 software (GraphPad software Inc, San Diego, CA). A P value of 0.05 or less was considered significant.

RESULTS

Expression of H_1R^R does not complement EAE in H_1R deficient mice

Using transgenic complementation, we recently showed that expression of the H_1R^S allele only in T cells of H1RKO mice was sufficient to restore EAE severity to WT levels in these mice (11). To understand if the H_1R^R allele would also complement EAE in H1RKO mice, we generated transgenic mice expressing the N-terminus hemagglutinin (HA)-tagged H_1R^R allele under the control of the distal *lck* promoter, which drives expression in peripheral T cells (14). The transgenic founders were generated directly on the C57BL/6J background and were crossed to H1RKO mice to obtain H1RKO mice expressing the H_1R^R allele selectively in T cells. The expression of the transgene in CD4 T cells was assessed by RT-PCR using transgene-specific primers (Fig. 1a) and by real time RT-PCR using primers that recognize H_1R (Fig. 1b). The two established lines of H_1R^R (H1RKO-Tg^R1 and H1RKO-Tg^R2) expressed the transgene mRNA at levels comparable to one of the H_1R^S allele transgenic mice (H1RKO-Tg^S) that we reported previously (11).

We then examined the susceptibility of these transgenic mice to myelin oligodendrocyte glycoprotein peptide 35–55 ($MOG_{35–55}$) induced EAE. We used two protocols to induce disease, one using $MOG_{35–55}$ plus complete Freund's adjuvant (CFA) and pertussis toxin (PTX) ($MOG_{35–55}$-CFA plus PTX) (Fig. 1c) and the other using two injections of $MOG_{35–55}$ plus CFA (2× $MOG_{35–55}$-CFA) (Fig. 1d), which does not use PTX as an ancillary adjuvant. Regression analysis revealed that the clinical disease courses elicited by both induction protocols fit a Sigmoidal curve and that the clinical course of disease in two

independent lines of H1RKO–Tg^R mice was not different from that in H1RKO mice. However, as reported previously (11), the clinical course of EAE in H1RKO-Tg^S mice was significantly more severe than that of H1RKO mice and was equivalent to the disease course observed in WT mice. These results indicate that, unlike the H_1R^S allele, expression of the H_1R^R allele by H1RKO T cells does not complement EAE susceptibility.

An analysis of EAE-associated clinical quantitative trait variables from the two transgenic cohorts revealed that the mean day of onset (DO), cumulative disease score (CDS), overall severity index (SI) and the peak score (PS) were significantly different among the strains immunized with either $MOG_{35–55}$-CFA plus PTX or 2× $MOG_{35–55}$-CFA (Table 1). *Post hoc* multiple comparisons of each trait variable revealed that H1RKO-Tg^S mice were equivalent to WT mice while H1RKO-Tg^R mice were equivalent to H1RKO mice. Furthermore, for each trait, H1RKO-Tg^S and WT mice were significantly greater than H1RKO-Tg^R and H1RKO mice.

We next analyzed the *ex vivo* $MOG_{35–55}$ specific proliferative response of spleen and draining lymph node (DLN) cells from mice immunized with 2× $MOG_{35–55}$-CFA. Significant differences in proliferative responses were not detected among WT, H1RKO, H1RKO-Tg^S and H1RKO-Tg^R mice (data not shown). Since $MOG_{35–55}$-stimulated splenocytes from immunized-H1RKO mice exhibit an immune deviation from Th1 to Th2 response in *ex vivo* recall assays (7), we analyzed cytokine production by $MOG_{35–55}$-stimulated spleen and DLN cells from mice immunized with both EAE-induction protocols. With the classical $MOG_{35–55}$-CFA plus PTX protocol, as we observed previously (11), antigen-stimulated spleen and DLN cells from H1RKO-Tg^S mice produced significantly greater amounts of IFN-γ compared to H1RKO mice and at levels comparable to WT mice (Fig. 2a). In contrast, the levels of IFN-γ produced by antigen-stimulated spleen and DLN cells from the two lines of H1RKO-Tg^R mice were equivalent to those produced by H1RKO mice. Similarly, antigen-stimulated spleen and DLN cells from H1RKO-Tg^S mice produced IL-4 at levels comparable to WT mice while those from H1RKO-Tg^R mice were similar to H1RKO mice (Fig. 2b). Similar results for IFN-γ (Fig. 2c) and IL-4 (Fig. 2e) were observed for 2× $MOG_{35–55}$-CFA immunized mice.

Because IL-17 is considered to be an important effector cytokine in EAE (19), we examined IL-17 production by spleen and DLN cells following *ex vivo* stimulation with $MOG_{35–55}$. IL-17 production by WT, H1RKO, H1RKO-Tg^S and H1RKO-Tg^R mice immunized with $MOG_{35–55}$-CFA and PTX was not significantly different (Fig. 2c) among strains. In contrast, IL-17 production by $MOG_{35–55}$ stimulated spleen and DLN cells from animals immunized with 2× $MOG_{35–55}$-CFA differed significantly among the strains (Fig. 2f). Compared to WT mice, H1RKO mice produced significantly less IL-17, indicating that H_1R signaling regulates IL-17 production by T cells. Moreover, production of IL-17 by H1RKO-Tg^S mice was not significantly different from WT mice and IL-17 production by H1RKO-Tg^R mice was not significantly different from H1RKO mice (Fig. 2f). Taken together, like EAE, H_1R^R expression in H1RKO T cells does not complement cytokine production by these cells.

H_1R alleles activate $G\alpha_q$ and $G\alpha_{11}$ equally well *in vitro*

The above results suggest that, in contrast to the H_1R^S allele, the H_1R^R allele is not functional. To understand the mechanism by which the polymorphic residues of the H_1R^S and H_1R^R alleles influence H_1R function, we examined the predicted structural location for the three residues within H_1R. The three polymorphic residues reside within the third intracytoplasmic loop of H_1R (Fig 3a), which is the region frequently associated with recruitment and activation of downstream G proteins (12). We, therefore, examined whether the polymorphic residues distinguishing the H_1R^S and H_1R^R alleles might result in significant alterations in G protein activation. Since H_1R is normally coupled to $G_{\alpha q}$ and/or $G_{\alpha 11}$ proteins, we generated fusion

proteins of the two H_1R alleles with both $G_{\alpha q}$ and $G_{\alpha 11}$ by linking in-frame the N-terminus of $G_{\alpha q/11}$ with the C-terminal tail of H_1R^R or H_1R^S.

HEK293 cells were transfected with the H_1R^S-$G\alpha_{q/11}$ or H_1R^R-$G\alpha_{q/11}$ fusion proteins, lysed and membrane fractions prepared from these cells. These were used initially to measure the levels of expression of each construct via the specific binding of the H_1R antagonist [^{3}H] mepyramine. There were no differences in the levels of specific binding of [^{3}H]mepyramine between the various constructs, indicating that the polymorphisms did not alter total protein expression. Also, the binding affinity of [^{3}H]mepyramine was not different between the two alleles (Fig 3b). To study their differential capacity to activate $G\alpha_q$ and $G\alpha_{11,}$ membrane amounts containing exactly the same number of copies of each construct were employed in [^{35}S]GTPγS binding assays. A maximally effective concentration of histamine stimulated binding of [^{35}S]GTP S equally to $G\alpha_q$ or $G\alpha_{11}$ when each G protein was linked to either the H_1R^S or H_1R^R variants (Fig. 3c, Fig. 3d). The dose-response curves to histamine indicated that the potency of histamine is equivalent for each receptor variant (data not shown). These data indicate that the H_1R^S and H_1R^R alleles can activate these G proteins equally well and that the phenotypic difference associated with the H_1R alleles is not inherently a function of differential capability to activate $G\alpha_q$ or $G\alpha_{11.}$

H_1R alleles are differentially expressed on the cell surface

Specific mutations in the signaling domain of several GPCRs (e.g. vasopressin V2 receptor, rhodopsin) can interfere with their cell surface expression and are associated with disease (20). To determine if the polymorphisms in H_1R influence cell surface expression of the receptor, HA-H_1R^S or HA-H_1R^R expression vectors were used to transfect HEK293T cells. The expression of these receptors at the cell surface was then examined by Flow cytometric analysis using an anti-HA mAb. HA-H_1R^S was expressed at higher levels than HA-H_1R^R (Fig. 4a). The number of H_1R^S-positive cells (Fig. 4b) and the mean florescence intensity of H_1R^S were considerably higher than those of H_1R^R, (Fig. 4c) indicating that the two H_1R alleles are differentially expressed on the cell surface. We observed similar results when the H_1R^S and H_1R^R constructs were transfected into 721.221 B cells (data not shown).

In parallel, we examined the cell surface expression of H_1R^S and H_1R^R by confocal microscopy using anti-HA mAb in cells stained prior to permeabilization. The results confirmed higher expression of H_1R^S on the surface than H_1R^R (Fig. 4d). However, Western blot analysis of H_1R^S and H_1R^R expression in lysates of transfected HEK293T cells showed no difference in the amount of total protein present (Fig. 4e). Taken together, these data indicate that the polymorphic residues associated with the H_1R^S and H_1R^R haplotypes result in differential translocation of the receptor to the cell surface.

H_1R^R is retained in the endoplasmic reticulum

The Western blot results described above (Fig. 4e) suggest that the H_1R^S and H_1R^R alleles are expressed at similar levels but that the H_1R^R allele is largely retained in intracellular compartments instead of being trafficked to the cell surface. To investigate this possibility, HEK293T cells were transfected with HA-H_1R^S or HA-H_1R^R constructs. After 24 h cells were fixed, permeabilized, stained with anti-HA mAb and observed by confocal microscopy. A predominantly plasma membrane staining pattern was observed for the H_1R^S allele (Fig. 5a). In contrast, a large fraction of the H_1R^R allele appeared to localize intracellularly (Fig. 5b) indicating that H_1R^R is retained in the intracellular compartments and fails to traffic efficiently to the cell surface. The network-like intracellular distribution of H_1R^R throughout the cell (Fig. 5b, right panel) resembled that of endoplasmic reticulum (ER). Therefore, to determine if the H_1R^R allele is retained in this compartment, we transiently co-transfected HEK293T cells with H_1R^S or H_1R^R constructs and a plasmid expressing the dsRed fluorescent protein that targets

the ER. Co-localization of the two proteins was examined by confocal microscopy following staining the cells for HA-H_1R. The majority of H_1R^R was again expressed intracellularly and co-localized with the dsRed protein, while minimal colocalization of H_1R^S with the ER-targeted dsRed protein was observed (Fig. 5b). Using LSM5 image browser software, we quantified the number of pixels that express both dsRed protein and HA-H_1R in multiple cells that were imaged under exactly the same settings. The results showed a significant difference in the co-localization of the H_1R^S and H_1R^R alleles in ER (Fig. 5c), suggesting that the H_1R^R L-M-S haplotype leads to its sequestration and retention in ER.

Retention of H_1R^R in the ER requires the L-M-S haplotype

To understand which of the three amino acids comprising the H_1R^R L-M-S haplotype is responsible for the observed differential cell surface expression of the allele we generated single H_1R^S mutants, replacing each of the H_1R^S haplotype associated residues with the corresponding H_1R^R allele (P263L, V312M, and P330S), by site directed mutagenesis. HEK293T cells were transfected with H_1R^S, H_1R^R and each of the three H_1R^S mutant constructs. Cells were stained with anti-HA mAb, without permeabilization, and cell surface expression of H_1R analyzed by Flow- cytometry. Each of the single H_1R^S mutants was expressed at higher levels on the cell surface than the H_1R^R allele (Fig. 6a) with the levels comparable to those observed with the H_1R^S allele. This indicates that the presence of a single H_1R^R polymorphism is not sufficient to induce its intracellular retention. We also generated double mutants of the H_1R^S allele wherein we replaced two residues of the H_1R^S haplotype with the corresponding residues of the H_1R^R allele (P263L and V312M, P263L and P330S, V312M and P330S). Similar to the single H_1R^S mutants, the double H_1R^S mutants were expressed on the cell surface at levels comparable to the H_1R^S and at significantly higher levels than the H_1R^R allele (Fig. 6b). We observed similar results in 721.221 B cells following transient transfection with H_1R^S, H_1R^S mutants and H_1R^R constructs (data not shown). Furthermore, when HEK293T cells were co-transfected with double H_1R^S mutants and the dsRed plasmid, each of the mutants showed a typical plasma membrane expression pattern with very little co-localization with the ER-targeted dsRed protein (Fig. 6c). Quantification of the number of pixels expressing dsRed- protein and HA-H_1R confirmed that each of the double H_1R^S mutants behaved like H_1R^S and only H_1R^R was retained in ER (Fig. 6d), confirming the flow cytometry data that all the polymorphic residues are required for differential cell surface expression of the H_1R alleles. Taken together, these data indicate that all three residues of the H_1R^R L-M-S haplotype are required for its intracellular sequestration. Interestingly, we sequenced the H_1R alleles from more than 100 different inbred laboratory and wild-derived mouse strains and did not identify any recombinant haplotypes suggesting that the two alleles are evolutionarily conserved and may have been selected functionally (data not shown).

DISCUSSION

To date, *Hrh1*/H_1R is the only murine EAE and EAO susceptibility gene that has been positionally cloned (7). In this study, using transgenic mouse models, we show that polymorphic variants in H_1R regulate cytokine production by T cells thereby influencing susceptibility to EAE. Furthermore, using HEK293T cells, we show that the polymorphisms in H_1R affect its functions by modulating cell surface expression rather than inherently altering the capacity of the receptor to generate intracellular signals.

Hrh1/H_1R has long been implicated in EAE susceptibility (7,8). As H_1R is widely expressed (10), this suggested that it might act in different cell types and at multiple checkpoints. We recently showed, however, that H_1R expression in T cells is sufficient to complement EAE severity in H1RKO mice. In this study, we show that the polymorphic residues of the H_1R^R allele interfere with its ability to complement EAE in H1RKO mice. This is in accordance with

genetic complementation studies in F1 hybrids between H1RKO and strains of mice expressing the H_1R^S or H_1R^R alleles. Susceptibility to histamine sensitivity could be restored in F1 hybrids of H1RKO and SJL/J, 129X1/SvJ or C57BL/6J that express H_1R^S allele but not in F1 hybrids between H1RKO and C3H/HeJ or CBA/J mice that express H_1R^R (7).

Hrh1/H_1R also controls delayed type hypersensitivity (DTH) responses when PTX is used as an adjuvant. The DTH response is mediated by CD4 T cells that produce large amounts of IFN-γ (21–23). Using C3H. *Bphs*^{S} congenic mice expressing the H_1R^S allele from SJL/J mice on the resistant C3H/HeJ background, Gao et al., (24) showed that polymorphisms in H_1R regulate ovalbumin-specific DTH response elicited in mice immunized with ovalbumin in CFA and PTX, indicating that the polymorphisms in H_1R regulate IFNγ production by CD4 T cells. This study confirms the role of H_1R polymorphisms in regulating IFN-γ production by these cells. Further, the complementation of IFN-γ production by splenocytes immunized using the 2× $MOG_{35–55}$ model suggests that H_1R regulation of IFNγ production by T cells does not require PTX.

Recently, IL-17-producing Th17 CD4 T cells have been considered more pathogenic in EAE (19). We show here, for the first time, that H_1R signaling regulates IL-17 production and that H_1R polymorphisms influence IL-17 production by T cells. However, it is noteworthy that we did not observe differences in IL-17 production between WT and H1RKO mice immunized with $MOG_{35–55}$-CFA plus PTX, nor in Th17 cells differentiated *in vitro* in the presence of excessive amounts of IL-6. PTX promotes the generation of Th17 cells, by inducing IL-6 production (25). Thus, it is possible that immunization with PTX (*in vivo*) or addition of exogenous IL-6 (*in vitro*) enables CD4 T cells to overcome the absence of H_1R signals required for the optimal IL-6 production and generation of Th17 cells. Even though we observed significant differences in IL-17 production by spleen and DLN cells from transgenic mice selectively expressing either H_1R^S or H_1R^R in T cells, we believe, based on *in vitro* differentiation data, that the H_1R regulation of IL-6 and IL-17 is independent of H_1R signals in T cells. In this regard, compared to WT macrophages H1RKO macrophages produce significantly less IL-6 (unpublished data) and treatment of lung parenchymal macrophages with H_1R blockers results in decreased IL-6 production (26). Further studies are being carried out to elucidate the role of H_1R in the generation of Th17 CD4 T cells.

GPCRs, in spite of the diversity of their polypeptide sequences, as a family retain enough structural information to allow them to be properly folded in the ER and adopt their highly conserved seven transmembrane confirmation (27). Several studies have identified critical residues and motifs important in many of the functions of GPCRs including ligand binding, G protein coupling, internalization, downregulation and intracellular trafficking (28). However, the three polymorphic residues distinguishing the H_1R^S and H_1R^R alleles are located in the third intracytoplasmic loop and do not constitute any known motif. Even though the exact PXXP motif is not present, it is worth noting that two of the three polymorphic residues associated with the H_1R^S haplotype are prolines, and that proline rich-motifs are known to mediate protein-protein interactions with Src homology SH3 domains (29). In this regard, polymorphic residues containing polyproline motifs in the third intracytoplasmic loop of the dopamine D4 receptor and β1-adrenergic receptor have been shown to interact with multiple SH3 domain-containing proteins (30) and affect the trafficking of these receptors. However, at this point, we do not have any evidence to suggest that H_1R interacts with any of the known SH3 domain-containing proteins or that such interactions differ between H_1R^S and H_1R^R alleles. Future studies will address this issue.

GPCRs interact with numerous proteins that play a role in their cellular trafficking (12). H_1R has an unusually long third intracytoplasmic loop, suggesting that the polymorphic residues may result in improper folding of the receptor to a non-native conformation in ER, which is

then recognized by the quality control machinery of molecular chaperones and excluded from ER export. Several chaperone proteins [such as Nina (31,32), ODR-4 (33,34) and a variety of receptor activity modifying proteins (RAMPs) (35,36)] that support the trafficking of a range of GPCRs to their target site have been identified. Therefore, it is possible that polymorphic residue-induced misfolding of H_1R^R could hinder its interaction with an essential chaperone thereby affecting its trafficking.

Proper cell surface expression of GPCRs is required to access the requisite ligands and signal transduction machinery (12). The functional importance of proper GPCR localization is emphasized by several human diseases that result from receptor mutation and mislocalization, including X-linked nephogenic diabetes, retinitis pigmentosa and hypogonadotrophic hypogonadism, which result from intracellular accumulation of mutant V2 vasopressin receptor, rhodopsin and gonadotropin releasing hormone receptor, respectively (20). In fact, mutations that lead to intracellular accumulation comprise the largest class of mutations in GPCRs that result in human diseases (12). Accordingly, our results are the first to demonstrate that structural polymorphisms influencing differential trafficking and cell surface expression of a GPCR in T cells can regulate immune functions and susceptibility to autoimmune disease.

Acknowledgements

Supported by the National Institutes of Health Grants AI041747, AI058052, AI045666, NS036526, and AI051454 and by National Multiple Sclerosis Society grant RG--3575.

References

1. Greenstein JI. Current concepts of the cellular and molecular pathophysiology of multiple sclerosis. Dev Neurobiol 2007;67:1248–1265. [PubMed: 17514718]
2. Hafler DA, Slavik JM, Anderson DE, O'Connor KC, De Jager P, Baecher-Allan C. Multiple sclerosis. Immunol Rev 2005;204:208–231. [PubMed: 15790361]
3. Kantarci O, Wingerchuk D. Epidemiology and natural history of multiple sclerosis: new insights. Curr Opin Neurol 2006;19:248–254. [PubMed: 16702830]
4. Gold R, Hartung HP, Toyka KV. Animal models for autoimmune demyelinating disorders of the nervous system. Mol Med Today 2000;6:88–91. [PubMed: 10652482]
5. Kuchroo VK, Anderson AC, Waldner H, Munder M, Bettelli E, Nicholson LB. T cell response in experimental autoimmune encephalomyelitis (EAE): role of self and cross-reactive antigens in shaping, tuning, and regulating the autopathogenic T cell repertoire. Annu Rev Immunol 2002;20:101–123. [PubMed: 11861599]
6. Andersson A, Karlsson J. Genetics of experimental autoimmune encephalomyelitis in the mouse. Arch Immunol Ther Exp (Warsz) 2004;52:316–325. [PubMed: 15507872]
7. Ma RZ, Gao J, Meeker ND, Fillmore PD, Tung KS, Watanabe T, Zachary JF, Offner H, Blankenhorn EP, Teuscher C. Identification of Bphs, an autoimmune disease locus, as histamine receptor H1. Science 2002;297:620–623. [PubMed: 12142541]
8. Linthicum DS, Frelinger JA. Acute autoimmune encephalomyelitis in mice. II. Susceptibility is controlled by the combination of H-2 and histamine sensitization genes. J Exp Med 1982;156:31–40. [PubMed: 6806429]
9. Teuscher C. Experimental allergic orchitis in mice. II. Association of disease susceptibility to the locus controlling Bordetella pertussis-induced sensitivity to histamine. Immunogenetics 1985;22:417–425. [PubMed: 4065933]
10. Parsons ME, Ganellin CR. Histamine and its receptors. Br J Pharmacol 2006;147(Suppl 1):S127–135. [PubMed: 16402096]
11. Noubade R, Milligan G, Zachary JF, Blankenhorn EP, del Rio R, Rincon M, Teuscher C. Histamine receptor H1 is required for TCR-mediated p38 MAP kinase activation and IFN-gamma productioin. J Clin Invest 2007;117:3507–3518. [PubMed: 17965772]

12. Tan CM, Brady AE, Nickols HH, Wang Q, Limbird LE. Membrane trafficking of G protein-coupled receptors. Annu Rev Pharmacol Toxicol 2004;44:559–609. [PubMed: 14744258]
13. Banu Y, Watanabe T. Augmentation of antigen receptor-mediated responses by histamine H1 receptor signaling. J Exp Med 1999;189:673–682. [PubMed: 9989982]
14. Wildin RS, Garvin AM, Pawar S, Lewis DB, Abraham KM, Forbush KA, Ziegler SF, Allen JM, Perlmutter RM. Developmental regulation of lck gene expression in T lymphocytes. J Exp Med 1991;173:383–393. [PubMed: 1988541]
15. Bakker RA, Dees G, Carrillo JJ, Booth RG, Lopez-Gimenez JF, Milligan G, Strange PG, Leurs R. Domain swapping in the human histamine H1 receptor. The Journal of pharmacology and experimental therapeutics 2004;311:131–138. [PubMed: 15159444]
16. Mitchell FM, Mullaney I, Godfrey PP, Arkinstall SJ, Wakelam MJ, Milligan G. Widespread distribution of Gq alpha/G11 alpha detected immunologically by an antipeptide antiserum directed against the predicted C-terminal decapeptide. FEBS letters 1991;287:171–174. [PubMed: 1908788]
17. Butterfield RJ, Sudweeks JD, Blankenhorn EP, Korngold R, Marini JC, Todd JA, Roper RJ, Teuscher C. New genetic loci that control susceptibility and symptoms of experimental allergic encephalomyelitis in inbred mice. J Immunol 1998;161:1860–1867. [PubMed: 9712054]
18. Teuscher C, Noubade R, Spach K, McElvany B, Bunn JY, Fillmore PD, Zachary JF, Blankenhorn EP. Evidence that the Y chromosome influences autoimmune disease in male and female mice. Proc Natl Acad Sci U S A 2006;103:8024–8029. [PubMed: 16702550]
19. Furuzawa-Carballeda J, Vargas-Rojas MI, Cabral AR. Autoimmune inflammation from the Th17 perspective. Autoimmun Rev 2007;6:169–175. [PubMed: 17289553]
20. Tao YX. Inactivating mutations of G protein-coupled receptors and diseases: structure-function insights and therapeutic implications. Pharmacol Ther 2006;111:949–973. [PubMed: 16616374]
21. Sewell WA, Munoz JJ, Vadas MA. Enhancement of the intensity, persistence, and passive transfer of delayed-type hypersensitivity lesions by pertussigen in mice. J Exp Med 1983;157:2087–2096. [PubMed: 6304228]
22. Sewell WA, Munoz JJ, Scollay R, Vadas MA. Studies on the mechanism of the enhancement of delayed-type hypersensitivity by pertussigen. J Immunol 1984;133:1716–1722. [PubMed: 6206132]
23. Sewell WA, de Moerloose PA, Hamilton JA, Schrader JW, Mackay IR, Vadas MA. Potentiation of delayed-type hypersensitivity by pertussigen or cyclophosphamide with release of different lymphokines. Immunology 1987;61:483–488. [PubMed: 3127325]
24. Gao JF, Call SB, Fillmore PD, Watanabe T, Meeker ND, Teuscher C. Analysis of the role of Bphs/Hrh1 in the genetic control of responsiveness to pertussis toxin. Infect Immun 2003;71:1281–1287. [PubMed: 12595443]
25. Chen X, Howard OM, Oppenheim JJ. Pertussis toxin by inducing IL-6 promotes the generation of IL-17-producing CD4 cells. J Immunol 2007;178:6123–6129. [PubMed: 17475838]
26. Triggiani M, Gentile M, Secondo A, Granata F, Oriente A, Taglialatela M, Annunziato L, Marone G. Histamine induces exocytosis and IL-6 production from human lung macrophages through interaction with H1 receptors. J Immunol 2001;166:4083–4091. [PubMed: 11238657]
27. Spiegel AM, Weinstein LS. Inherited diseases involving g proteins and g protein-coupled receptors. Annu Rev Med 2004;55:27–39. [PubMed: 14746508]
28. Duvernay MT, Filipeanu CM, Wu G. The regulatory mechanisms of export trafficking of G protein-coupled receptors. Cell Signal 2005;17:1457–1465. [PubMed: 16014327]
29. Sparks AB, Hoffman NG, McConnell SJ, Fowlkes DM, Kay BK. Cloning of ligand targets: systematic isolation of SH3 domain-containing proteins. Nat Biotechnol 1996;14:741–744. [PubMed: 9630982]
30. Oldenhof J, Vickery R, Anafi M, Oak J, Ray A, Schoots O, Pawson T, von Zastrow M, Van Tol HH. SH3 binding domains in the dopamine D4 receptor. Biochemistry 1998;37:15726–15736. [PubMed: 9843378]
31. Shieh BH, Stamnes MA, Seavello S, Harris GL, Zuker CS. The ninaA gene required for visual transduction in Drosophila encodes a homologue of cyclosporin A-binding protein. Nature 1989;338:67–70. [PubMed: 2493138]
32. Schneuwly S, Shortridge RD, Larrivee DC, Ono T, Ozaki M, Pak WL. Drosophila ninaA gene encodes an eye-specific cyclophilin (cyclosporine A binding protein). Proc Natl Acad Sci U S A 1989;86:5390–5394. [PubMed: 2664782]

33. Dwyer ND, Troemel ER, Sengupta P, Bargmann CI. Odorant receptor localization to olfactory cilia is mediated by ODR-4, a novel membrane-associated protein. Cell 1998;93:455–466. [PubMed: 9590179]

34. Gimelbrant AA, Haley SL, McClintock TS. Olfactory receptor trafficking involves conserved regulatory steps. J Biol Chem 2001;276:7285–7290. [PubMed: 11060288]

35. McLatchie LM, Fraser NJ, Main MJ, Wise A, Brown J, Thompson N, Solari R, Lee MG, Foord SM. RAMPs regulate the transport and ligand specificity of the calcitonin-receptor-like receptor. Nature 1998;393:333–339. [PubMed: 9620797]

36. Christopoulos A, Christopoulos G, Morfis M, Udawela M, Laburthe M, Couvineau A, Kuwasako K, Tilakaratne N, Sexton PM. Novel receptor partners and function of receptor activity-modifying proteins. J Biol Chem 2003;278:3293–3297. [PubMed: 12446722]

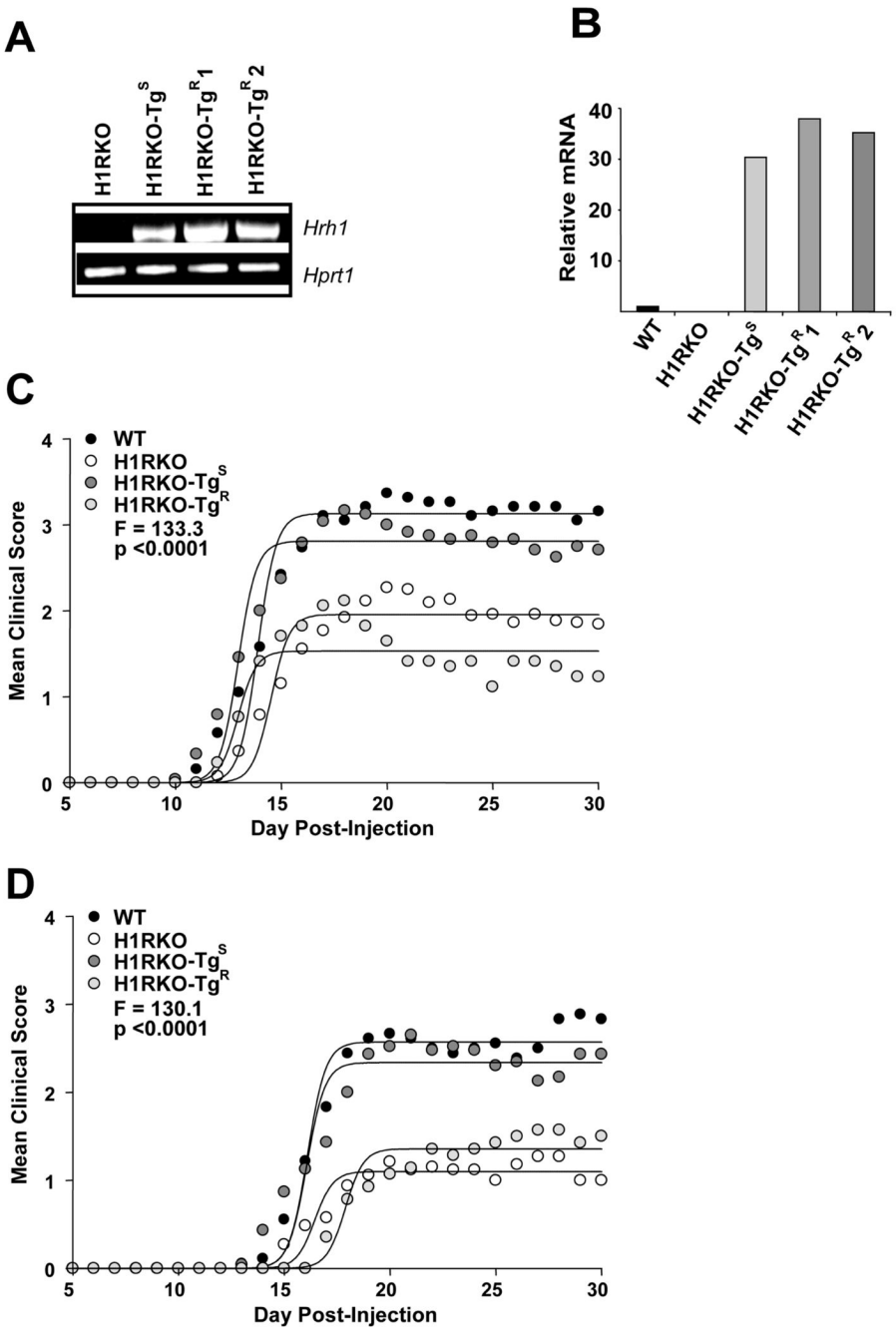

Figure 1.

Transgenic expression of the H_1R^R allele in H1RKO T cells fails to complement EAE in H1RKO mice. H_1R transgene expression was analyzed by (**a**) RT-PCR and (**b**) quantitative RT-PCR in CD4 T cells from H1RKO mice and transgenic mice expressing the H_1R^S or H_1R^R allele that were crossed with H1RKO mice (H1RKO-Tg^S, H1RKO-Tg^R1 and H1RKO-Tg^R2). H1RKO-Tg^R1 and H1RKO-Tg^R2 represent two independent lines. (**c**) Clinical EAE in WT (n = 19), H1RKO (n = 56), H1RKO-Tg^S (n = 24), and H1RKO-Tg^R (n = 17) mice that were immunized with $MOG_{35–55}$-CFA plus PTX. Mice were scored daily starting at D5. Regression analysis revealed that the disease course elicited fits a Sigmoidal curve and that the clinical disease course of the animals was significantly different among the strains. The clinical

disease courses of WT and H1RKO-Tg^S mice were both significantly more severe than those of H1RKO-Tg^R and H1RKO mice ($P < 0.0001$ for all comparisons). (**d**) WT (n = 18), H1RKO (n = 33), H1RKO-Tg^S (n = 23), and H1RKO-Tg^R (n = 14) mice were immunized with 2× $MOG_{35–55}$-CFA. EAE severity was significantly different among the strains. The clinical disease courses of WT and H1RKO-Tg^S mice were both significantly more severe than those of H1RKO-Tg^R and H1RKO mice ($P < 0.0001$ for all comparisons).

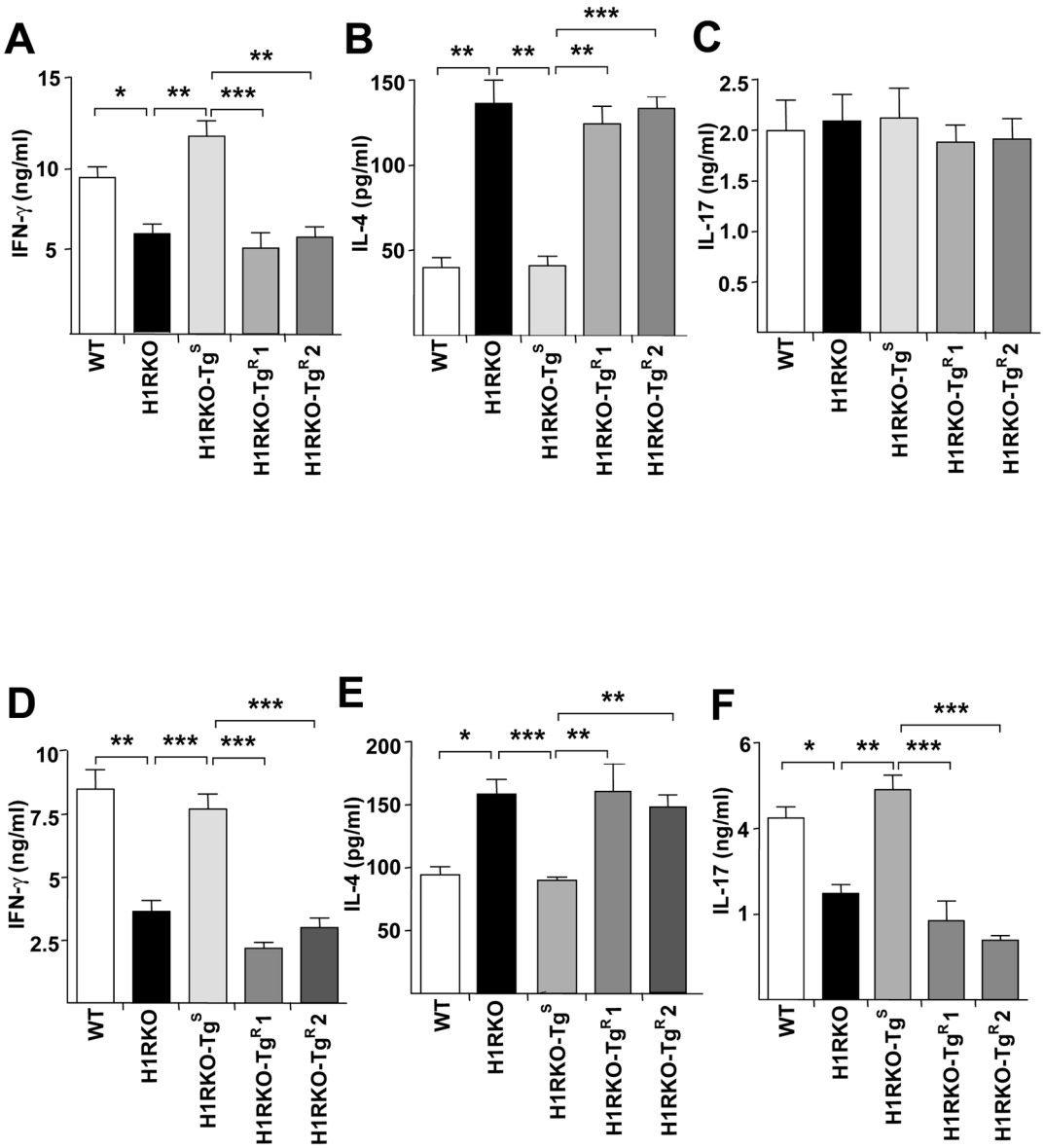

Figure 2.

Transgenic expression of H_1R^R in H1RKO T cells fails to complement cytokine production by H1RKO mice. (**a–c**) Spleen and draining lymph node (DLN) cells were isolated from $MOG_{35–55}$-CFA plus PTX-immunized WT, H1RKO, H1RKO-Tg^S and H1RKO-Tg^R mice 10 days post immunization and stimulated with 50 μg/ml of $MOG_{35–55}$ for 72h (n=4–8 mice per group). Supernatants were collected and analyzed for the production of IFN-γ (**a**), IL-4 (**b**) and IL-17 (**c**). Significance of differences in cytokine production were assessed by Kruskal-Wallis statistical analysis followed by Dunn's post-hoc multiple comparisons (Kruskal-Wallis statistic = 25.73; $p < 0.0001$ for IFNγ, Kruskal-Wallis statistic = 31.34; $p < 0.0001$ for IL-4, Kruskal-Wallis statistic = 0.514; $p > 0.5$ for IL-17. * $p< 0.05$ ** $p<0.01$ and *** $p<0.001$). (**d-f**) Spleen and DLN cells from 2× $MOG_{35–55}$-CFA immunized mice were collected on day 10 post immunization and were activated with 50μg/ml of $MOG_{35–55}$ for 72h, supernatants were collected and analyzed for IFN-γ (**d**), IL-4 (**e**) and IL-17 (**f**) by ELISA in triplicate. Significance of differences in cytokine production were assessed by Kruskal-Wallis statistical analysis

followed by Dunn's post-hoc multiple comparisons (Kruskal-Wallis statistic = 52.23; $p < 0.0001$ for IFNγ, Kruskal-Wallis statistic = 23.88; $p < 0.0001$ for IL-4, Kruskal-Wallis statistic = 35.22; $p < 0.0001$ for IL-17. * $p< 0.05$ ** $p<0.01$ and *** $p<0.001$). Data are presented as the mean ± SEM and are representative of two independent experiments.

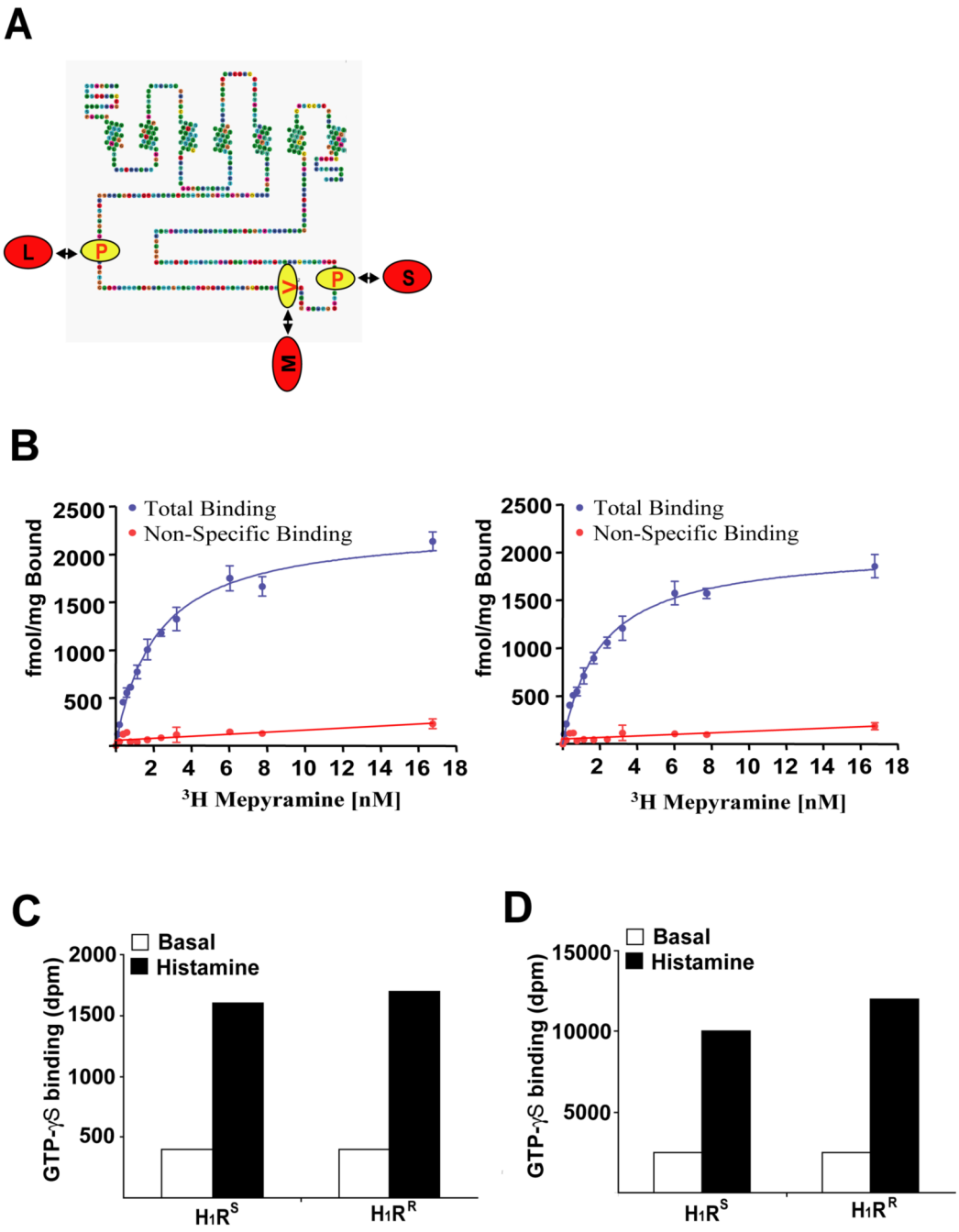

Figure 3.

H_1R^S and H_1R^R activate $G\alpha_{q/11}$ G proteins equally well. (**a**) The amino acid sequence of the mouse histamine receptor H_1 is displayed with differences between the H_1R^R allele (Red) and the H_1R^S allele (Yellow) highlighted. Each of the sites of variation is within the long, third intracellular loop. (**b**) Saturation [^{3}H]mepyramine binding studies were performed on membranes of HEK293T cells transfected to express a $H_1R^-G\alpha_q$ fusion protein (left hand side H_1R^R, right hand side H_1R^S). Non-specific binding was determined in the same manner but with the additional presence of 1μM mianserin. Data are presented as the mean ± SEM. These studies provided quantitation of construct expression levels. (**c** and **d**) membranes containing 50 fmol of H_1R^S or H_1R^R linked to either $G\alpha_q$ (**c**) or $G\alpha_{11}$ (**d**) were used in [^{35}S]GTPγS binding

studies conducted in the absence (basal, open bars) or presence (histamine, filled bars) of 100 μM histamine to assess the capability of the two variants to activate the G proteins. H_1R^S and H_1R^R were equi-effective in causing activation of each G protein. Representative data from four independent experiments are shown.

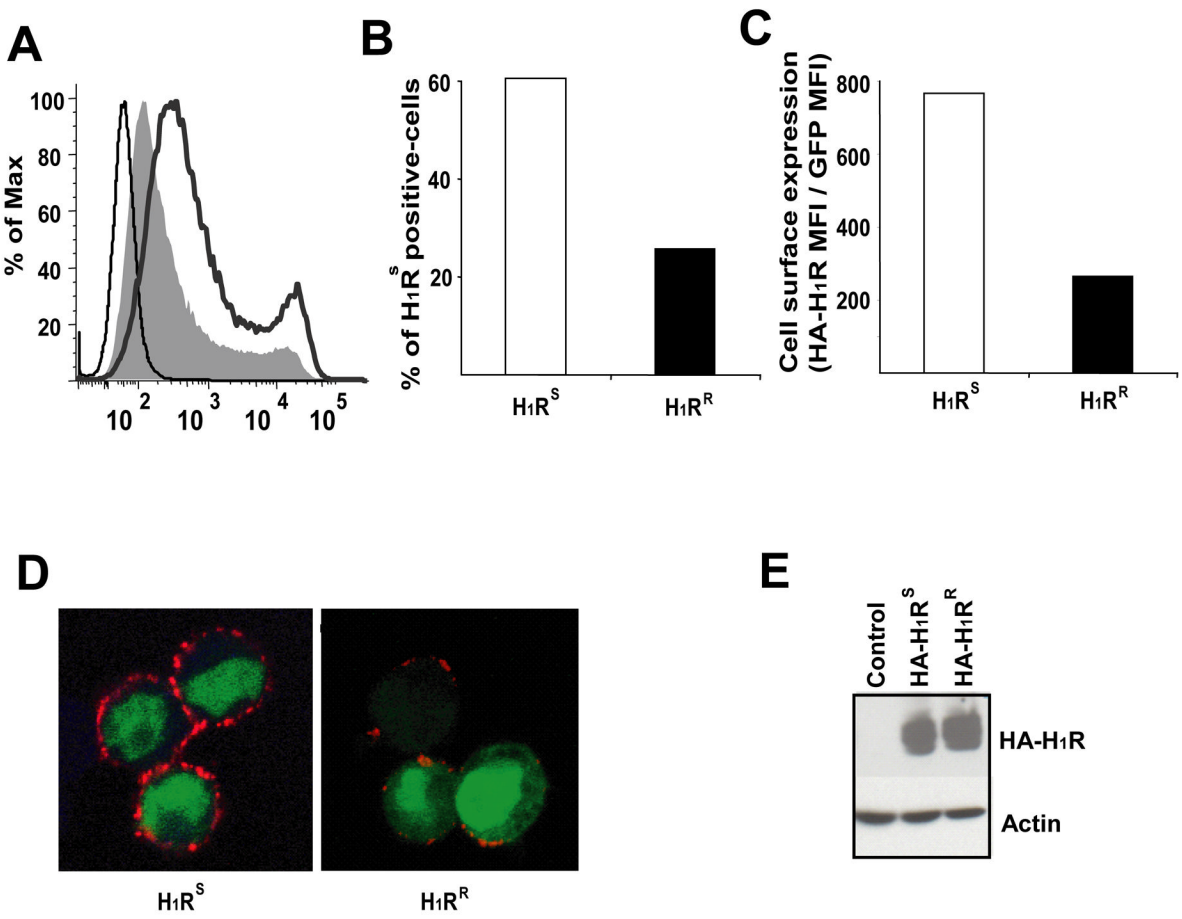

Figure 4.

H_1R^S and H_1R^R alleles are differentially expressed on the cell surface. (**a**) HEK293T cells were transfected with empty pEGZ, pEGZ-HA-H_1R^S or pEGZ-HA-H_1R^R plasmids. Cells were collected 16–24h later without trypisinization, stained with anti-HA mAb and analyzed by Flow cytometry. The thin line represents cells transfected with empty pEGZ whereas the thick line represents cells transfected with HA-H_1R^S and the filled area represents cells transfected with HA-H_1R^R. (**b & c**) HEK293T cells were analyzed as in (**a**) and the percentage (**b**) and the mean florescence intensity (MFI) of anti-HA on H_1R^S positive cells (**c**) were determined. (**d**) HEK293T cells transfected with HA-H_1R^S or HA-H_1R^R plasmids and 24 h later cells were stained with anti-HA mAb (red) without permeabilization. Cells were visualized by confocal microscopy. GFP (green) is shown as a marker of transfected cells. (**e**) HEK293T cells were transfected as in (**a**), whole cell lysates prepared and analyzed by Western blotting using anti-HA mAb. Actin is shown as loading control. Representative data from three independent experiments are shown.

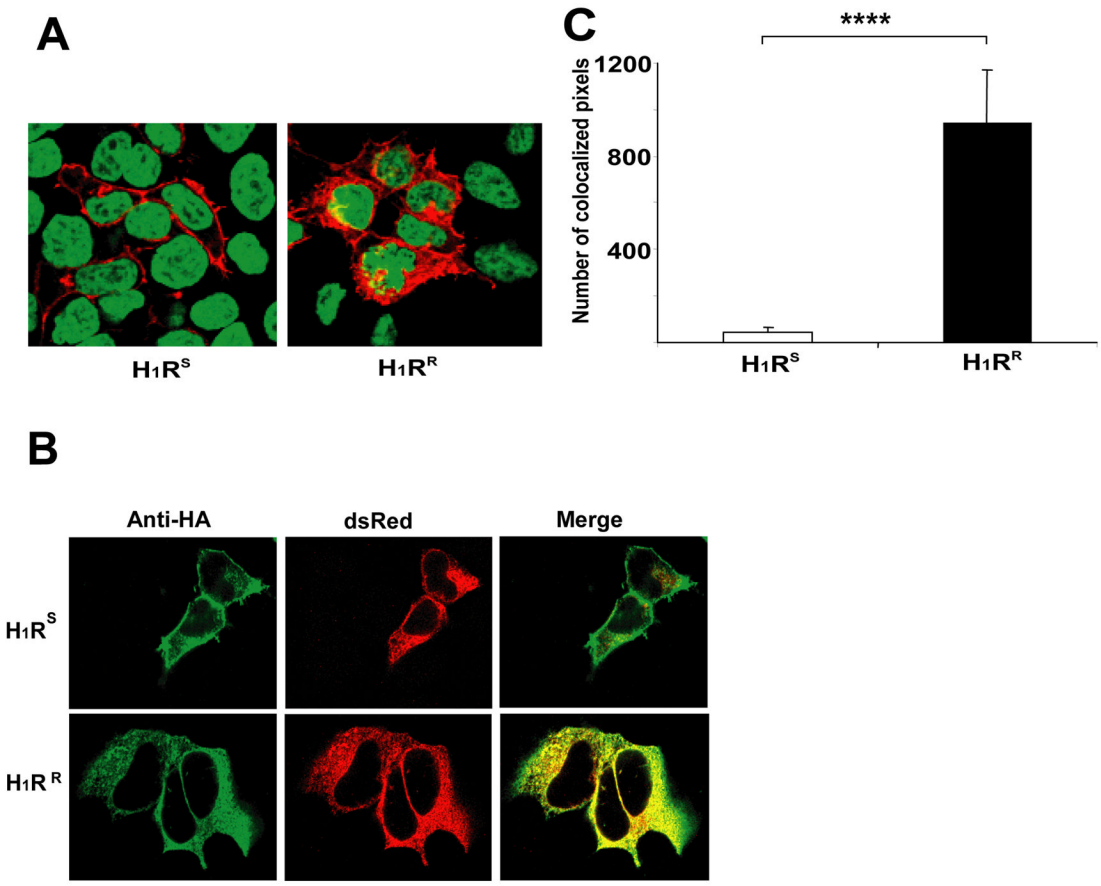

Figure 5.

H_1R^R is retained in the endoplasmic reticulum. (**a**) HEK293T cells were transfected with HA-H_1R^S or HA-H_1R^R plasmids. 24h later, cells were fixed, permeabilized, stained with anti-HA mAb (red) and TOPRO-3 nuclear stain (blue) and visualized by confocal microscopy. (**b**) HEK293T cells were co-transfected with pdsRed plasmid that express ER targeted florescent dsRed protein (red) and HA-H_1R^S or HAH_1R^R. 24h later cells were fixed, permeabilized, stained with anti-HA mAb (green) and the co-localization of HA-H_1R with dsRed was visualized by confocal microscopy. Yellow color represents the co-localization of red and green colors. (**c**) Quantification of HA-H_1R co-localization with dsRed protein. Using Zeiss LSM 510 META Confocal imaging software, the numbers of pixels expressing both colors were determined ($n \geq 26$) and the data is presented as the average of number of pixels that co-express dsRed and HA-H_1R. Error bars represent SEM. Data were analyzed using Mann-Whitney statistical test (Mann-Whitney U = 133.0 **** $p<0.00001$).

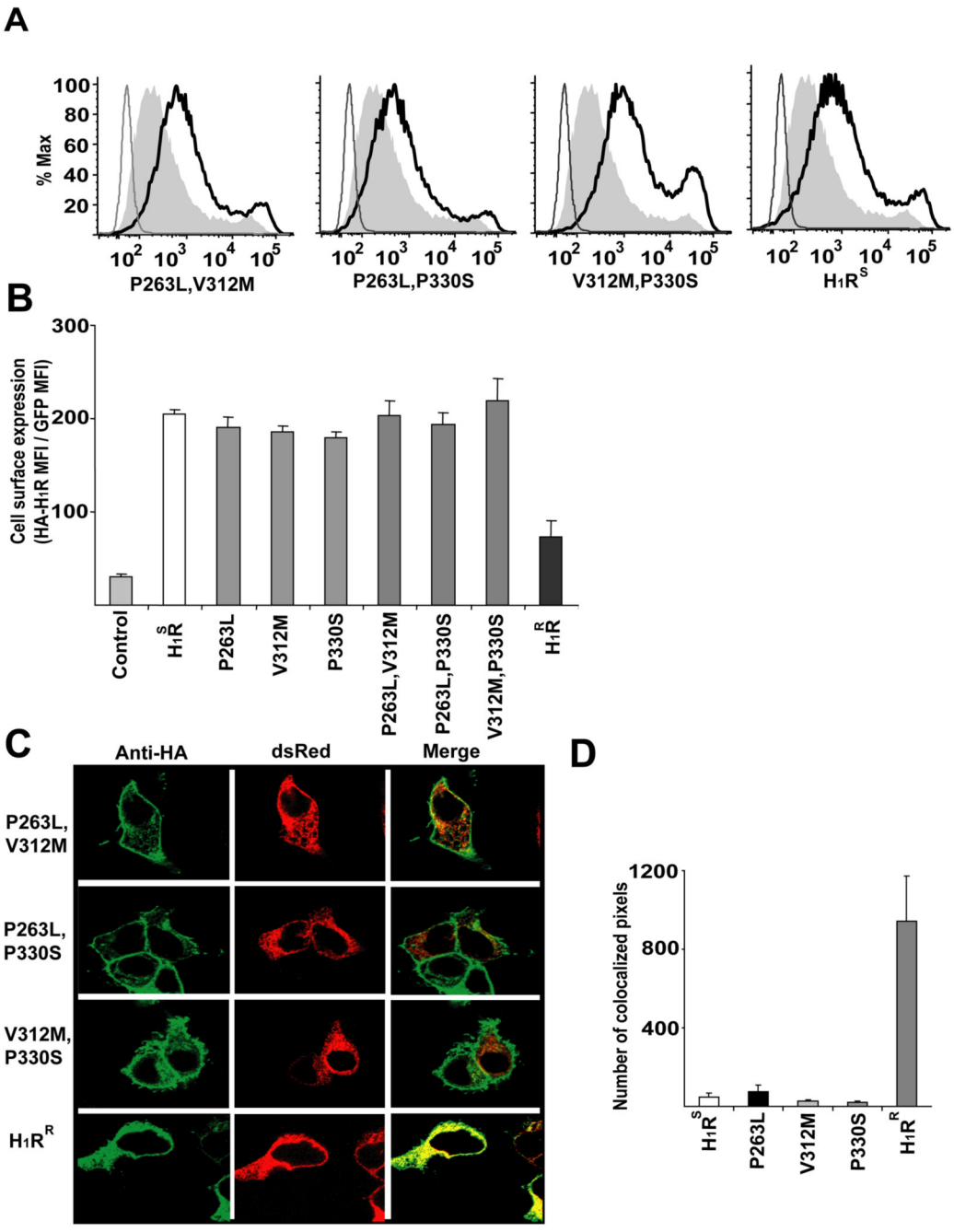

Figure 6.

ER retention of the H_1R^R allele requires the L-M-S haplotype. (**a**) HEK293T cells were transfected with empty control, single HA-H_1R^S mutants or HA-H_1R^R plasmids. Cells were collected 16–24 h later without trypisinization, stained with anti-HA mAb and analyzed by flow cytometry. Cells transfected with HA-H_1R^S are shown as positive controls in the far-right panel. The thin line represents cells transfected with empty pEGZ whereas the thick line represents cells transfected with HA-H_1R^S and the filled area represents cells transfected with HA-H_1R^R. (**b**) HEK293T cells were analyzed as in (**a**) and the mean florescence intensity of anti-HA on H_1R^S positive cells was determined. The data presented is the average of triplicate transfections. (**c**) HEK293T cells were co-transfected with pdsRed plasmid that express ER

targeted dsRed protein (red) and HA-H_1R^S, mutants of HA-H_1R^S or HA-H_1R^R. 24h later, cells were fixed, permeabilized, stained with anti-HA mAb (green) and the co-localization of HA-H_1R with dsRed (red) was visualized by confocal microscopy. Yellow color represents the co-localization of red and green colors. (**d**) Quantification of HA-H_1R co-localization with dsRed protein. Using Zeiss LSM 510 META Confocal imaging software the number of pixels expressing both the colors was determined in a number of cells ($n \geq 16$) and the data is presented as the average of number of pixels that co-express dsRed and HA-H_1R. Error bars indicate SEM.

Table 1

Clinical disease traits following immunization of mice with $MOG_{35–55}$-CFA plus PTX (A) or 2× $MOG_{35–55}$-CFA (B)

(a) **Strain**	**Incidence**	**DO**	**CDS**	**SI**	**PS**
C57BL/6J	19/19	13.1±0.3	56.2±4.6	3.1±0.2	3.9±0.3
H1RKO	55/56	15.7±0.4	32.1±1.4	2.1±0.1	3.0±0.1
H1RKO-Tg^S	24/24	12.9±0.4	50.0±3.7	2.8±0.2	3.6±0.2
H1RKO-Tg^R	16/17	13.3±0.3	28.6±2.3	1.7±0.1	2.4±0.2
	$\chi^2 = 2.5$	F = 13.5	21.2	19.2	14.4
	p = 0.5	p < 0.0001	< 0.0001	< 0.0001	< 0.0001
			C57BL/6J = H1RKO-Tg^S ≠ H1RKO-Tg^R= H1RKO		
(b)					
Strain	Incidence	DO	CDS	SI	PS
C57BL/6J	18/18	16.6±0.7	37.6±2.9	2.6±0.1	3.2±0.2
H1RKO	26/33	17.1±0.5	20.0±1.8	1.6±0.1	2.2±0.1
H1RKO-Tg^S	22/23	16.2±0.6	36.4±3.8	2.5±0.2	3.2±0.2
H1RKO-Tg^R	13/14	18.7±0.6	18.6±3.1	1.6±0.2	1.9±0.2
	$\chi^2 = 7.4$	F = 2.8	11.6	15.2	14.0
	p = 0.06	p = 0.05	< 0.0001	< 0.0001	< 0.0001
			C57BL/6J = H1RKO-Tg^S ≠ H1RKO-Tg^R= H1RKO		